XV, 84433-40-9; *meso*-tetraphenylporphyrin-2-*trans*-acrylic acid, 77698-95-4; 4-amino-2,2,6,6-tetramethyl-1-oxypiperidine, 14691-88-4; 3-amino-2,2,5,5-tetramethyl-1-oxy-pyrrolidine, 34272-83-8; *meso*-tetraphenylporphyrin-2-*cis*-acrylic acid, 77629-57-3; *meso*-tetra-

phenylporphyrin-2-propanoic acid, 83037-22-3; copper(II) *meso*-tetraphenyl-2-formylporphyrin, 71763-49-0; 3-isocyanato-2,2,5,5-tetramethyl-1-oxypyrroline, 68212-42-0; 2-carboxy-12,17-diethyl-3,7,8,13,18-pentamethylporphyrin, 43012-54-0.
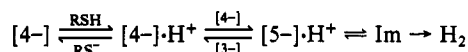
The Homogeneous Hydrogen-Evolving Systems $[Mo_2Fe_6S_8(SPh)_9]^{4-,5-}/C_6H_5SH$: Reaction Characteristics, Kinetics, and Possible Mechanisms

T. YAMAMURA,[1a] G. CHRISTOU,[1b] and R. H. HOLM*

The reduced clusters $[Mo_2Fe_6S_8(SPh)_9]^{4-,5-}$ ([4–], [5–]) and $[Fe_4S_4(SPh)_4]^{3-}$ evolve H_2 from benzenethiol in solutions of purified N,N'-dimethylacetamide at ambient temperature. With 500 equiv of thiol clusters [4–] and [5–] afford 86% and $\sim 100\%$ H_2 yields, respectively, after 24 h. Cluster [5–] also produces H_2 from a variety of other protic sources including an 83% yield from 2 equiv of Et_3NH^+ after 24 h. Both [5–]/PhSH and [4–]/PhSH systems generate a common intermediate (Im), which is the last kinetically resolvable species prior to H_2 evolution, experimentally expressible as $d[H_2]/dt = K[Im][PhSH]$. Analysis of H_2 evolution rates in the [4–]/PhSH system leads to the experimental rate law $d[H_2]/dt = [4-]^2[PhSH]^2/\{2300([3-] + 0.00043)[PhS^-] + 0.014[PhSH]\}$. The kinetics of a large number of reaction schemes were theoretically analyzed. Acceptable schemes are those that conform to the preceding rate laws and other experimental constraints. From these the simplest chemically reasonable schemes are proposed for Im formation in the [5–]/PhSH system and H_2 evolution in the [4–]/PhSH system. The latter is considered to be

$$[4-] \underset{RS^-}{\overset{RSH}{\rightleftharpoons}} [4-]\cdot H^+ \underset{[3-]}{\overset{[4-]}{\rightleftharpoons}} [5-]\cdot H^+ \rightleftharpoons Im \rightarrow H_2$$

involving cluster protonation, electron transfer, Im formation, and H_2 evolution. The reaction sequence is presumably driven by the demonstrated irreversibility of the overall reaction $2[4-] + 2PhSH \rightarrow 2[3-] + 2PhS^- + H_2$. Details of the kinetic analysis and alternative schemes are presented. The potential advantage of a two-electron carrier for reduction of H^+ (to hydride) and other two-electron substrates is noted. In this work this advantage is expressed in the proposed and alternative reaction schemes and is experimentally demonstrated by a 42% H_2 yield from the one-electron reductant $[Fe_4S_4(SPh)_4]^{3-}$ and ~ 500 equiv of PhSH after 24 h.

Introduction

Hydrogenases are uni- or bidirectional catalysts of reaction 1 in the presence of a suitable electron carrier $C_{ox,red}$. This and subsequent reactions are collected in Table I. Characterization of these enzymes,[2,3] which contain Fe–S cluster(s)[4] that presumably function as internal electron-transfer sites and/or the catalytic center itself, is clearly in an accelerating phase. While the enzyme kinetics of several hydrogenases have been elucidated, little is known of reaction mechanisms at a molecular basis other than the intervention of enzyme–hydride intermediates.[3] Consequently, kinetic and mechanistic investigations of stoichiometric and catalytic $2H^+/H_2$ processes effected by well-defined metal species could provide information pertinent to an eventually satisfactory description of enzyme action.

Activation of dihydrogen by the uptake reaction eq 2, involving heterolytic cleavage to form a metal hydride and often facilitated by a general base B, is a well-developed subject.[5–7]

The formation of HD in the reverse reaction of systems containing D_2 and a protic solvent with complexes of, e.g., Ag(I), Cu(II), and Ru(III),[5,7–9] constitutes strong evidence for hydride formation. In contrast, spontaneous dihydrogen evolution from a protic source HA by a reducing metal complex or cluster (not introduced as a preformed hydride) in homogenous solutions has received substantially less attention. Synthetic, homogeneous, dihydrogen-evolving systems of this sort have been described,[10–15] several of which are based on unidentified Fe–S–SR species,[11,14] but kinetic and mechanistic details are lacking. Dihydrogen formation by reactions 3, in which M is a mono- or polynuclear species capable of two-electron transfer to substrate, is likely in these cases. In the Ru(bpy)$_3^0$/CH$_3$CN/D$_2$O system the detection of D_2, and no HD from H atom abstraction from acetonitrile by D·, is consistent with a hydride intermediate.[13] Further evidence for such

(1) (a) On leave from Department of Chemistry, Faculty of Science, University of Tokyo. (b) U.K. Science Research Council/NATO Postdoctoral Fellow, 1980–1981.
(2) Schlegel, H. G.; Schneider, K., Eds. "Hydrogenases: Their Catalytic Activity, Structure, and Function"; Erich Goltze KG: Göttingen, 1978.
(3) Adams, M. W. W.; Mortenson, L. E.; Chen, J.-S. *Biochim. Biophys. Acta* 1981, *594*, 105.
(4) Several hydrogenases recently have been found to contain nickel: Albracht, S. P. J.; Graf, E.-G.; Thauer, R. K. *FEBS Lett.* 1982, *140*, 311. LeGall, J.; Ljungdahl, P. O.; Moura, I.; Peck, H. D., Jr.; Xavier, A. V.; Moura, J. J. G.; Teixera, M.; Huynh, B. H.; DerVartanian, D. V. *Biochem. Biophys. Res. Commun.* 1982, *106*, 610.
(5) James, B. R. "Homogeneous Hydrogenation"; Wiley: New York, 1973.
(6) James, B. R. *Adv. Organomet. Chem.* 1979, *17*, 319.

(7) Brothers, P. J. *Prog. Inorg. Chem.* 1981, *28*, 1.
(8) (a) Webster, A. H.; Halpern, J. *J. Phys. Chem.* 1957, *61*, 1239. (b) Schindewolf, U. *Ber. Bunsenges. Phys. Chem.* 1963, *67*, 219. (c) von Hahn, H. E. A.; Peters, E. *J. Phys. Chem.* 1971, *75*, 571.
(9) Harrod, J. F.; Cicconi, S.; Halpern, J. *Can. J. Chem.* 1966, *39*, 1372.
(10) Christensen, R. J.; Espenson, J. H.; Butcher, A. B. *Inorg. Chem.* 1973, *12*, 564.
(11) Tano, K.; Schrauzer, G. N. *J. Am. Chem. Soc.* 1975, *97*, 5404.
(12) Nikonova, L. A.; Isaeva, S. A.; Pershikova, N. I.; Shilov, A. E. *J. Mol. Catal.* 1975/1976, *1*, 367.
(13) Abruña, H. D.; Teng, A. Y.; Samuels, G. J.; Meyer, T. J. *J. Am. Chem. Soc.* 1979, *101*, 6746.
(14) Okura, I.; Nakamura, S.; Nakamura, K.-I. *J. Mol. Catal.* 1979, *6*, 71. Okura, I.; Nakamura, S. *Ibid.* 1980, *9*, 125. Okura, I.; Nakamura, S.; Kobayashi, M. *Bull. Chem. Soc. Jpn.* 1981, *54*, 3794.
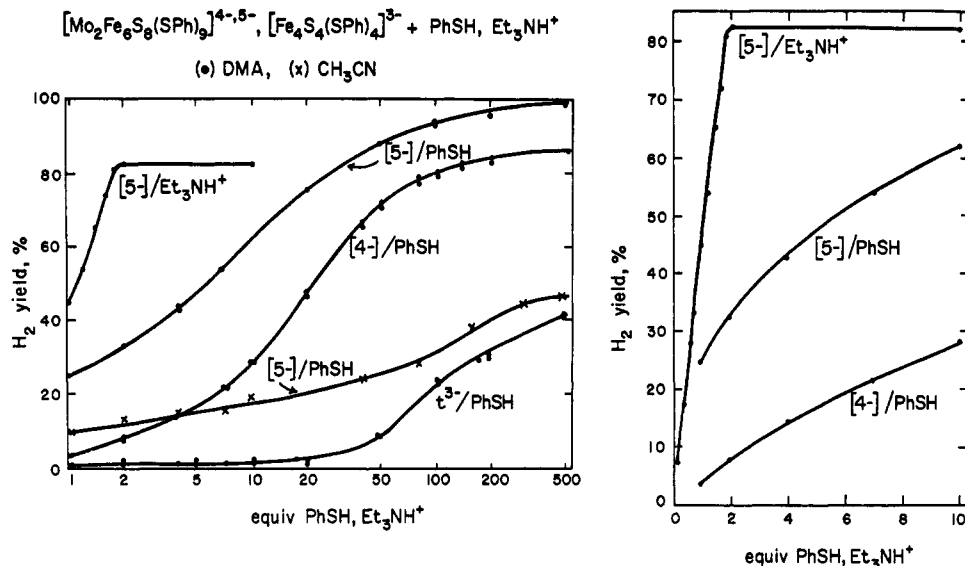(15) Schrauzer, G. N.; Palmer, M. R. *J. Am. Chem. Soc.* 1981, *103*, 2659.

Table I. Reactions Pertinent to H_2 Evolution and Uptake

no.	reaction
1	$2H^+ + 2C_{red} \underset{H_2ase}{\rightleftharpoons} H_2 + 2C_{ox}$
2	$H_2 + M^{n+} + B \rightleftharpoons M^{n+}-H^- + BH^+$
3	$HA + M^{n+} \rightarrow M^{(n+2)+}-H^- + A^-$ $M^{(n+2)+}-H + HA \rightarrow M^{(n+2)+} + H_2 + A^-$
4	$H\cdot + M^{n+} \rightarrow M^{(n+1)+}-H^- \xrightarrow{H_3O^+} M^{(n+1)+} + H_2$
5	$[Mo_2Fe_6S_8(SR)_9]^{3-} \underset{-1.02\ V}{\overset{E_1}{\rightleftharpoons}} [Mo_2Fe_6S_8(SR)_9]^{4-} \underset{-1.23\ V}{\overset{E_2}{\rightleftharpoons}}$ $[Mo_2Fe_6S_8(SR)_9]^{5-}$
6	$[Mo_2Fe_6S_8(SPh)_9]^{5-} + 2PhSH \rightarrow [Mo_2Fe_6S_8(SPh)_9]^{3-} + H_2 + 2PhS^-$
7	$2[Fe_4S_4(SPh)_4]^{3-} + 2PhSH \rightarrow 2[Fe_4S_4(SPh)_4]^{2-} + H_2 + 2PhS^-$
8	$[Mo_2Fe_6S_8(SPh)_9]^{3-} + [Mo_2Fe_6S_8(SPh)_9]^{5-} \rightleftharpoons 2[Mo_2Fe_6S_8(SPh)_9]^{4-}$
9	$2[Mo_2Fe_6S_8(SPh)_9]^{4-} + 2PhSH \rightarrow 2[Mo_2Fe_6S_8(SPh)_9]^{3-} + H_2 + 2PhS^-$
10	$[Mo_2Fe_6S_8(SPh)_9]^{5-} + 2Et_3NH^+ \rightarrow [Mo_2Fe_6S_8(SPh)_9]^{3-} + H_2 + 2Et_3N$
11	$[5-] + PhSH \rightleftharpoons Im$
12a	$[4-] + PhSH \rightleftharpoons Im'$
12b	$2[4-] + PhSH \rightleftharpoons Im + [3-]$

Scheme I

20a	$[5-] + PhSH \underset{k_2}{\overset{k_1}{\rightleftharpoons}} [5-]\cdot PhSH$
20b	$[5-]\cdot PhSH \underset{k_4}{\overset{k_3}{\rightleftharpoons}} [5-]\cdot H^+ + PhS^-$
20c	$[5-]\cdot H^+ \underset{k_6}{\overset{k_5}{\rightleftharpoons}} Im$

Scheme II

22a	$[4-] + PhSH \underset{k_2}{\overset{k_1}{\rightleftharpoons}} [4-]\cdot H^+ + PhS^-$
22b	$[4-]\cdot H^+ + [4-] \underset{k_4}{\overset{k_3}{\rightleftharpoons}} [5-]\cdot H^+ + [3-]$
22c	$[5-]\cdot H^+ \underset{k_6}{\overset{k_5}{\rightleftharpoons}} Im$
22d	$Im + PhSH \xrightarrow{k_7} [3-] + PhS^- + H_2$

intermediates is found in the oxidation of hydrogen atoms by metal ions in aqueous solution,[16] reaction 4. In several systems transient hydride species, including $FeH^{2+,16c}$ have been detected.

The double-cubane complexes $[Mo_2Fe_6S_8(SR)_9]^{3-}$ (**1**) have

$$[Mo_2Fe_6S_8(SR)_9]^{3-,4-,5-}$$

1 [3-], **2** [4-], **3** [5-]

occupied a central role in the continuing development of Mo–Fe–S cluster chemistry,[17-22] an appreciable portion of

which is directed toward modeling the Mo atom coordination unit in nitrogenase.[17] In the present context the most interesting feature of these complexes is the electron-transfer series (5), consisting of two chemically reversible steps,[19,21,22b] yielding the reduced clusters **2** and **3**. Potentials vs. SCE for the R = Ph system in DMF solution[19] are given. One example of **3**, $(Et_4N)_5[Mo_2Fe_6S_8(SPh)_9]$, has been isolated and characterized.[19] Thus **3** presents the uncommon property, shared with $Ru(bpy)_3^0$, of a single molecule carrying two low-potential electrons that could be delivered to substrate as in, e.g., reaction 3. This possibility has been realized in the form of reaction 6, which in N,N'-dimethylacetamide solution proceeds to completion in ≤24 h in the presence of a large excess of benzenethiol.[23] Under the same conditions the one-electron carrier $[Fe_4S_4(SPh)_4]^{3-}$[24] $(E(2-/3-) = -1.04$ V in DMF) gave only $\leq30\%$ yield of H_2 based on reaction 7.[23] In the present investigation these observations have been extended and elaborated in a detailed examination of, primarily, the H_2-evolving systems $[Mo_2Fe_6S_8(SPh)_9]^{4-,5-}/PhSH$. A treatment of the kinetics of H_2 evolution is presented together with probable reaction mechanisms.

Experimental Section

Preparation of Compounds. $(n\text{-}Bu_4N)_3[Mo_2Fe_6S_8(SPh)_9]$,[22a] $(Et_4N)_5[Mo_2Fe_6S_8(SPh)_9]$,[19] $(Et_4N)_2[Fe_4S_4(SPh)_4]$,[25] $(Et_4N)_3$-$[Fe_4S_4(SPh)_4]$,[24] and $(Et_4N)(SPh)$[18] were synthesized by published methods. Benzenethiol-$2,4,6$-d_3 was prepared as outlined[26] starting from aniline-$2,4,6$-d_3.[27] The crude product was reduced by $LiAlH_4$ in ether solution to remove traces of disulfide and was hydrolyzed by aqueous HCl under argon. The ethereal fraction was dried over CaH_2, and the thiol was purified by distillation. Benzenethiol-S-d (PhSD) was obtained by the reaction of NaSPh with 35% DCl/D_2O followed by anaerobic extraction with ether and fractional distillation. $(Et_3NH)(PF_6)$ was prepared by treatment of 5.5 g of $(Et_3NH)Cl$ with 6.7 g of $NaPF_6$ in 200 mL of acetone followed by removal of NaCl by filtration and solvent evaporation. Recrystallization of the residue from dichloromethane afforded the product (90%) as a white crystalline solid.

Purification of Reagents and Solvents. All operations were carried out under a pure argon atmosphere. Commercial benzenethiol was refluxed overnight over CaH_2 (40 mesh, 10 g/200 mL) and was fractionally distilled twice at atmospheric pressure; only the middle fractions ($\sim20\%$ of the distillate) were retained in each distillation. Commercial samples of t-BuSH, $PhCH_2SH$, m-$CF_3C_6H_4SH$,[28] and 1,3-propanedithiol were purified similarly. p-Chlorobenzenethiol, p-toluenethiol, phenol, and catechol were sublimed. Trifluoroacetic acid was twice distilled, with 80% second fractions retained in each step. Other reagents were of analytical grade and were not further purified.

Commercial N,N'-dimethylacetamide (DMA, Aldrich or Eastman Kodak Spectrograde) was dried over two separate batches of Linde 4-Å molecular sieves, refluxed for 3 days over freshly opened CaH_2, and then separated from the latter by filtration. The filtrate was stirred with 1.5 g of sodium acenaphthylenide/100 mL (generated in situ by using acenaphthylene recrystallized from methanol) for 24 h at ambient temperature, and the mixture was distilled at reduced pressure. (In this and subsequent distillation steps the pot temperature was kept

(16) (a) Czapski, G.; Jortner, J.; Stein, G. *J. Phys. Chem.* **1961**, *65*, 960. (b) Schwarz, H. A. *Ibid.* **1963**, *67*, 2827. (c) Jayson, G. G.; Keene, J. P.; Stirling, D. A.; Swallow, A. J. *Trans. Faraday Soc.* **1969**, *65*, 2453. (d) Behar, D.; Samuni, A. *Chem. Phys. Lett.* **1973**, *22*, 105. (e) Cohen, H.; Meyerstein, D. *J. Chem. Soc., Dalton Trans.* **1974**, 2559. (f) Mićić, O. I.; Nenadović, M. T. *Ibid.* **1979**, 2001. (g) Nenadović, M. T.; Mićić, O. I.; Muk, A. A. *Ibid.* **1980**, *586*. (h) Ryan, D. A.; Espenson, J. A. *Inorg. Chem.* **1981**, *20*, 4401.

(17) Holm, R. H. *Chem. Soc. Rev.* **1981**, *10*, 455.

(18) Palermo, R. E.; Power, P. P.; Holm, R. H. *Inorg. Chem.* **1982**, *21*, 173.

(19) Christou, G.; Mascharak, P. K.; Armstrong, W. H.; Papaefthymiou, G. C.; Frankel, R. B.; Holm, R. H. *J. Am. Chem. Soc.* **1982**, *104*, 2820.

(20) Wolff, T. E.; Berg, J. M.; Hodgson, K. O.; Frankel, R. B.; Holm, R. H. *J. Am. Chem. Soc.* **1979**, *101*, 4140.

(21) Wolff, T. E.; Power, P. P.; Frankel, R. B.; Holm, R. H. *J. Am. Chem. Soc.* **1980**, *102*, 4694.

(22) (a) Christou, G.; Garner, C. D. *J. Chem. Soc., Dalton Trans.* **1980**, 2354. (b) Christou, G.; Garner, C. D.; Miller, R. M.; Johnson, C. E.; Rush, J. D. *Ibid.* **1980**, 2363.

(23) Christou, G.; Hageman, R. V.; Holm, R. H. *J. Am. Chem. Soc.* **1980**, *102*, 7600.

(24) Cambray, J.; Lane, R. W.; Wedd, A. G.; Johnson, R. W.; Holm, R. H. *Inorg. Chem.* **1977**, *16*, 2565.

(25) DePamphilis, B. V.; Averill, B. A.; Herskovitz, T.; Que, L., Jr.; Holm, R. H. *J. Am. Chem. Soc.* **1974**, *96*, 4159.

(26) Hagen, K. S.; Stephan, D. W.; Holm, R. H. *Inorg. Chem.* **1982**, *21*, 3928.

(27) Best, A. P.; Wilson, C. L. *J. Chem. Soc.* **1946**, 239.

(28) Wong, G. B.; Kurtz, D. M., Jr.; Holm, R. H.; Mortenson, L. E.; Upchurch, R. G. *J. Am. Chem. Soc.* **1979**, *101*, 3078.

$[Mo_2Fe_6S_8(SPh)_9]^{4-,5-}$, $[Fe_4S_4(SPh)_4]^{3-}$ + PhSH, Et$_3$NH$^+$

($\bullet$) DMA, (x) CH$_3$CN

Figure 1. H$_2$ evolution from PhSH and (Et$_3$NH)(PF$_6$) by reduced clusters in DMA ($\bullet$) and acetonitrile (X) solutions after 24-h reaction time. Initial concentrations: [5−], 0.99 mM; [4−] and [Fe$_4$S$_4$(SPh)$_4$]$^{3-}$ (t^{3-}), 1.98 mM. In this and subsequent figures equivalents of protic reactant and percent yield are expressed as described in the text. Equivalents in the left figure are plotted on a log scale.

below 40 °C and only the central 80% fraction of the distillate was retained.) The sodium acenaphthylenide/distillation step was performed two further times. Then the procedure beginning at the CaH$_2$ step was repeated. DMA purified in this way gave the absorbance ratio A_{400}/A_{480} = 3.72 for solutions of (Et$_4$N)$_5$[Mo$_2$Fe$_6$S$_8$(SPh)$_9$]. Only solvent batches affording this value (±0.02) were used in H$_2$-evolution systems. Acetonitrile and acetonitrile-d_3 were purified by a published method.[29]

H$_2$-Evolution Systems. The DMA solvent and all liquid reactants were thoroughly degassed before use. Reactions were conducted in vials under a pure argon atmosphere. In a typical run 0.80 mL of a 1.00 mM solution of (Et$_4$N)$_5$[Mo$_2$Fe$_6$S$_8$(SPh)$_9$] (or a 2.00 mM solution of [Mo$_2$Fe$_6$S$_8$(SPh)$_9$]$^{4-}$ or (Et$_4$N)$_3$[Fe$_4$S$_4$(SPh)$_4$]) in DMA was pipetted into a vial of known volume. The 4− cluster was generated by reaction 8, for which K_{eq} = 10$^{3.56}$,[19] using exactly equal concentrations of the initial clusters. Under this condition the mole fraction of the 4− cluster is 0.97. The desired amount of neat PhSH or PhSH/DMA solution was added to the vial through a serum cap by means of an airtight syringe. After maintenance at ∼25 °C for determined periods the reaction systems were quenched by the addition of 50 μL of 1.0 M PhSSPh in DMA, which causes immediate oxidation of reduced clusters. Analysis of H$_2$ was performed with a Varian Model 3700 gas chromatograph equipped with a 1-m column of Linde 5-Å molecule sieves. Argon was used as the carrier gas. Analysis of H$_2$-HD-D$_2$ mixtures was carried out with use of a 6-m column of activated alumina coated with iron(III) oxide that was immersed in a liquid-nitrogen bath.[30] The gases were converted to water over heated copper(II) oxide prior to analysis;[31] helium was used as the carrier gas.

The H$_2$-evolution propensity of [Mo$_2$Fe$_6$S$_8$(SPh)$_9$]$^{5-}$ in DMA solution was screened by using a variety of protic acids. The following results were obtained with a 2/1 acid/cluster mole ratio and 24-h reaction time; percent H$_2$ yields are based on the stoichiometry of reactions analogous to (6): H$_2$O, CH$_3$OH, PhOH, catechol, 0%; PhCO$_2$H, 9.7%; HOAc, 3.2%; CF$_3$CO$_2$H, 66%; (Et$_3$NH)(PF$_6$), 83%; m-CF$_3$C$_6$H$_4$SH, 26%; p-ClC$_6$H$_4$SH, PhSH, 32%; p-CH$_3$C$_6$H$_4$SH, 27%; HS(CH$_2$)$_3$SH, 37%; PhCH$_2$SH, 14%; t-BuSH, <1%. Reaction systems containing benzenethiol were selected for detailed study. In achieving reproducible H$_2$ yields in these systems, it was found necessary to employ thiol and DMA, which were purified as described. Use of DMA giving absorbance ratios lower than that specified led to decreased yields.

Physical Measurements. Absorption spectra were recorded on a Cary Model 219 spectrophotometer. ^{1}H NMR spectra (300 MHz) were measured with a Bruker WM-300 spectrometer; chemical shifts

downfield and upfield of Me$_4$Si reference are designated as negative and positive, respectively. Electrochemical measurements were made with standard Princeton Applied Research equipment using a glassy-carbon working electrode, a Ag/AgCl (0.1 M KCl) reference electrode, and 0.1 M (n-Pr$_4$N)(PF$_6$) supporting electrolyte. All measurements were performed under strictly anaerobic conditions with degassed solvents.

Results

In the following parts the clusters **1**, **2**, and **3** with R = Ph are designated as [3−], [4−], and [5−], respectively. Equivalents of protic reactant (HA) are defined in terms of the number of reduced clusters required for the formal reaction

$$H^+ \xrightarrow{2e^-} H^-$$
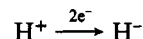
Thus, in reactions 6 and 10, 1 equiv of HA = 1 mol of HA/mol of [5−], and in reactions 7 and 9, 1 equiv of HA = 1 mol of HA/2 mol of [Fe$_4$S$_4$(SPh)$_4$]$^{3-}$ or [4−]. Percent yields of H$_2$ are based on moles of reduced clusters in these reactions. The oxidized clusters [3−] and [Fe$_4$S$_4$(SPh)$_4$]$^{2-}$ were inactive in all H$_2$-evolution assays.

H$_2$ Evolution by Reduced Clusters. Dihydrogen-evolving systems containing protic reactants HA, the two-electron reductant [5−], and the one-electron reductants [4−] and [Fe$_4$S$_4$(SPh)$_4$]$^{3-}$ have been sought, with the simultaneous restrictions that (i) the system remains homogeneous over the course of the reaction, (ii) cluster degradation is absent or minimal, allowing secure identification of the cluster oxidation product, and (iii) H$_2$ yields approach 100% at accessible HA/cluster mole ratios, indicating well-behaved reaction systems. In initial experiments it was found that, of the three reduced clusters, [5−] was the most effective in promoting H$_2$ evolution. Certain observations of systems containing this cluster were utilized to select the final system for detailed study.

Under the set of fixed conditions described in the Experimental Section ∼1 mM [5−] in DMA was observed to evolve H$_2$ from Et$_3$NH$^+$, three carboxylic acids, and six thiols. No H$_2$ was detected with HA = water, methanol, or phenol. With acids and thiols there is a rough correlation between decreasing aqueous pK_a[32] and increasing H$_2$ yield. Yields with the former are low except for that with CF$_3$CO$_2$H (66%). Use of larger amounts of these carboxylic acids tends to promote cluster

(29) Walter, M.; Ramaley, L. *Anal. Chem.* **1973**, *45*, 165.
(30) Moore, W. R.; Ward, H. R. *J. Phys. Chem.* **1960**, *64*, 832.
(31) Moore, W. R.; Ward, H. R. *J. Am. Chem. Soc.* **1958**, *80*, 2909.

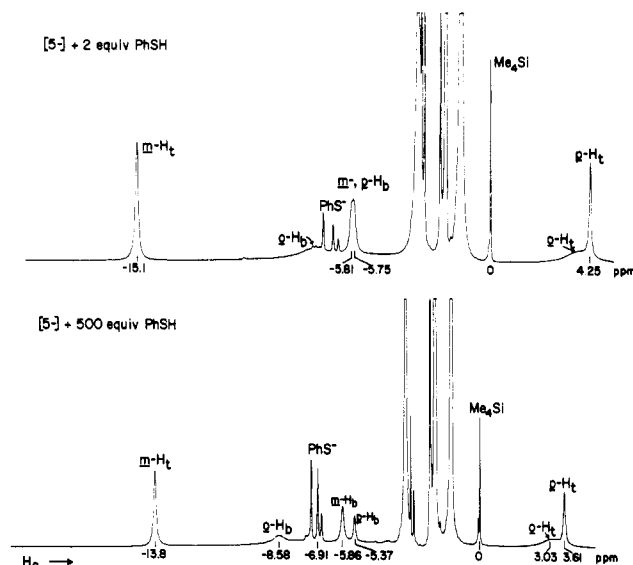(32) Danehy, J. P.; Parasmeswaran, K. N. *J. Chem. Eng. Data* **1968**, *13*, 386.

Figure 2. ^1H NMR spectra of reaction systems initially containing 0.99 mM [5-] + 2 equiv of PhSH after 2 h and +500 equiv of PhSH at completion of reaction ($\sim$20 hr). Reactions were conducted in DMA solution, the solvent and thiol were removed in vacuo, and the spectra of the residues were recorded in CD_3CN solutions. Signal assignments are indicated (t = terminal, b = bridging ligand). Cation and protio solvent peaks are unlabeled.

Figure 3. Time dependence of absorbance changes in the reaction system initially containing 1.98 mM [4-] + 50 equiv of PhSH in DMA solution (l = 0.008 98 cm): 0 (a), 3.3 min (b), 80 min (c), 240 min (d), 20 h (e); $\cdots\cdots$, 1.98 mM [3-]; $\cdots$, e – [3-] difference spectrum showing the formation of PhS$^-$. The points $\times$ represent the spectrum of this system calculated on the basis of 71% H_2 yield after 20 h and with the assumption that [3-] and [4-] are the only absorbing species at 400–600 nm.

decomposition. Yields with HA = RSH were variant (<1–37%). These systems are complicated by thiolate ligand substitution reactions[18] (R $\neq$ Ph), which alter redox potentials in series 5[19] and make unclear the exact nature of ligation during the H_2-evolution process. Such difficulties are absent when HA = PhSH. Shown in Figure 1 is the dependence of H_2 yield on equivalents of PhSH after 24-h reaction time. At 2 equiv a H_2 yield of 32% is found and at $\sim$500 equiv 100% yield is attained, confirming our earlier report.[23] With Et_3NH^+ H_2 evolution is more rapid than with PhSH and reaches 83% with only 2 equiv (Figure 1). At 10 equiv of Et_3NH^+ the yield is unchanged, an observation suggestive of cluster decomposition. The system [5-]/PhSH in acetonitrile exhibits substantially reduced yields over the 1–500-equiv range compared to this system in DMA. At 2 and 500 equiv of thiol the yields are 13% and 46%, respectively.

Both [4-] and $[Fe_4S_4(SPh)_4]^{3-}$ evolve H_2 from PhSH in DMA solutions. The yield curves in Figure 1 show that at equal equivalents (or PhSH/cluster mole ratios) these clusters are less efficient than [5-]. At 2 and 500 equiv of thiol H_2 yields are 7.7% and 86%, respectively, for [4-] and 1.2% and 42%, respectively, for $[Fe_4S_4(SPh)_4]^{3-}$. The latter value is $\sim$10% higher than that found previously,[23] a result presumably due to the use of more extensively purified DMA. No H_2 was detected in systems containing $[Fe_4S_4(SPh)_4]^{3-}$ and PhSH in acetonitrile or Et_3NH^+ in DMA.

On the basis of the foregoing observations and restrictions i–iii the systems [5-]/PhSH and [4-]/PhSH in DMA[33] were selected for further examination.

Overall Reactions in [4-]/PhSH and [5-]/PhSH Systems. Presented in Figure 2 are ^1H NMR spectra of the [5-]/PhSH system with 2 and 500 equiv of PhSH after 2 h and complete reaction, respectively. The spectrum of the 2-equiv case exhibits resonances of PhS$^-$ centered near −6.9 ppm and isotropically shifted resonances of bridging and terminal ligands in the clusters. Chemical shifts of the latter are intermediate of those of separately observed [4-] and [5-] in CD_3CN.[19]

owing to rapid electron exchange. Any [3-] formed would be discharged by reaction 8 inasmuch as the H_2 yield is <50% on the basis of initial [5-]. In the 500-equiv case the H_2 yield is $\sim$100%, the ligand chemical shifts are within ±0.05 ppm of those of authentic [3-] in CD_3CN,[19] and the m-H_t/PhS$^-$ intensity ratio is 1.2:1. These observations augment the earlier finding that the 450-nm band characteristic of [3-] appears in the spectrum of the [5-]/500-equiv PhSH system after completion of H_2 evolution.[23]

The time-dependent electronic spectral changes for the [4-]/PhSH system with 50 equiv of thiol are shown in Figure 3. Initial spectrum a ([4-]) is replaced by spectrum e after 20-h reaction time. The calculated spectrum, based on 71% yield of H_2 (Figure 1) from reaction 9, agrees to within 5% with spectrum e at 400–600 nm. The small discrepancy could arise from adventitious oxidation of [4-]. The difference spectrum e – [3-] at 270–400 nm reveals a well-defined peak at 310 nm, which is observed for $(Et_4N)(SPh)$ in DMA (ϵ_M^{310} 19 700 M^{-1} cm^{-1}). On the assumption that the spectrum of PhS$^-$ is not significantly perturbed by the exogenous thiol, the A_{310} value corresponds to formation of 0.75 mol of PhS$^-$/mol of [4-], in good agreement with the 71% H_2 yield. The 310-nm feature is absent in the corresponding difference spectrum of a [4-]/10-equiv Et_3NH^+ system, in which the reduced cluster is largely oxidized to [3-]. These observations support description of the *limiting* stoichiometries of H_2 evolution in the systems [5-]/PhSH and [4-]/PhSH as those of reactions 6 and 9, respectively.

Behavior of H_2-Evolution Reactions. Having established the stoichiometries of H_2 evolution in the [5-]/PhSH and [4-]/PhSH systems, we direct attention to certain features of these systems that are pertinent to kinetic analysis of the evolution reactions. Although the systems appear to be well-behaved, in terms of continued H_2 evolution, over longer periods, the observations refer to the first ca. 2–5 h of reaction. This is done to minimize any cluster degradation or adven-

---

(33) DMA was chosen as a suitable solvent on the basis of higher H_2 yields than in acetonitrile. An extensive study of the dependence of yield on solvent was not undertaken.
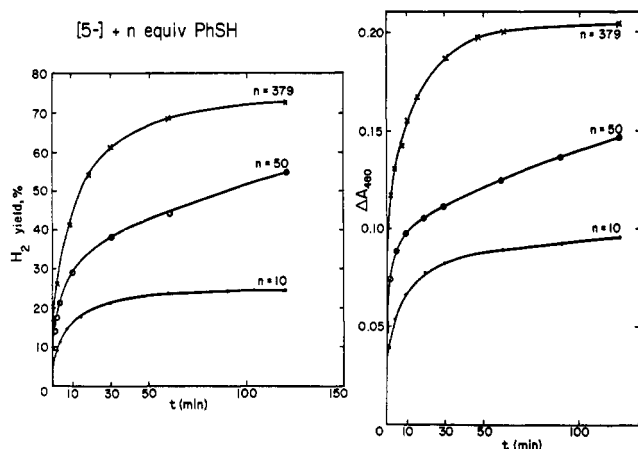
Figure 4. Time course of the reaction system initially containing 0.99 mM [5-] and n = 10, 50, 379 equiv of PhSH in DMA solutions, followed by H_2 yield (left) and absorbance change at 480 nm (right).
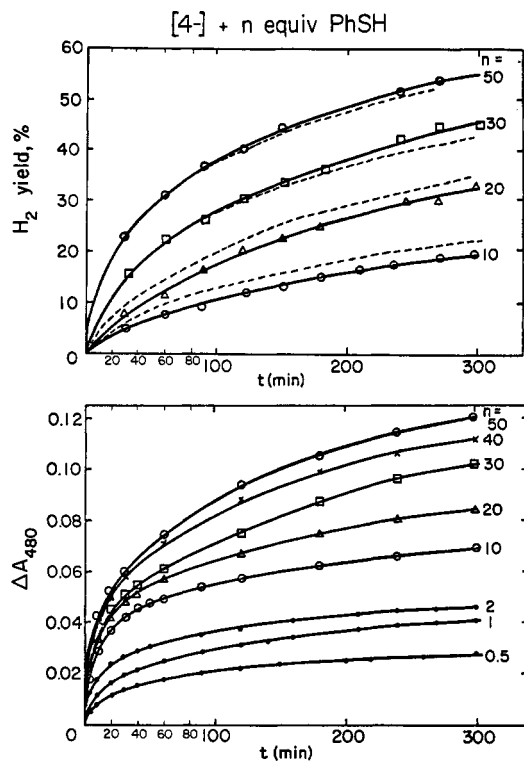

Figure 5. Time course of the reaction system initially containing 1.98 mM [4-] and n = 0.5-50 equiv of PhSH in DMA solutions, followed by H_2 yield (top) and absorbance change at 480 nm (bottom): - - -, H_2 yields calculated from integrated rate law for Scheme II, eq A-18.

Figure 6. Effect of H_2 yield in a reaction system initially containing 1.98 mM [4-] + 50 equiv of PhSH in DMA solution, to which were added [3-] (top) and PhS⁻ (bottom). The initial mole ratios of [3-] and PhS⁻ to [4-] are given.

titious oxidation and to render the kinetic treatment more tractable. At the ends of these times the observed H_2 yields are about half or more of those found with the same amount of thiol after 24 h (Figure 1).

(a) Source of H_2. In one experiment 1 mM [5-] in DMA was treated with ~500 equiv of PhSD and the system was allowed to react for 24 h. Gas chromatographic analysis showed the formation of D_2; no HD or H_2 was detected. Solutions of PhSH in DMA lacked the absorption band at 310 nm shown by $(Et_4N)(SPh)$ in the solvent. These results demonstrate that the source of H_2 (D_2) is molecular PhSH(D), other protic sources being negligible.

(b) Time Course. The dependence of H_2 yield on time with varying amounts of thiol in the [5-]/PhSH and [4-]/PhSH systems are depicted in Figures 4 and 5, respectively. Rates of H_2 formation increase with increasing amounts of thiol. Absorbance changes at 480 nm, where [5-], [4-], and [3-]

absorb appreciably[19] (Figure 3), track closely with the H_2 yield curves, indicating that these changes are related to the H_2-evolution reactions. This behavior at low amounts of thiol is utilized in the kinetic analysis.

(c) Inhibition. The appearance of [3-] and PhS⁻ as products of reactions 6 and 9 suggested an inhibitory effect on H_2 evolution by these species. Inhibition by both was verified in the system [4-]/50 equiv of PhSH, as shown by the data plotted in Figure 6. Yields of H_2 are decreased, up to at least 300-min reaction time, with the extent of inhibition increasing with increasing mole ratios of [3-] or PhS⁻ to initial [4-]. At the highest [3-]/[4-] and PhS⁻/[4-] ratios tested, the uninhibited H_2 yield at, e.g., 270 min (53%), is decreased by factors of 1.4 and 2.7, respectively. Because [3-] and [4-] do not chemically react (other than by electron exchange), nor do PhS⁻ and either cluster at the mole ratios examined, the inhibition arises from mass action effects on one or more of the elementary processes in H_2 evolution. If the evolution reaction is inhibited by H_2 itself, then the reverse of reactions 6 and 9 should occur. This matter was first examined with the systems [4-]/- and [5-]/50 equiv of PhSH. The absorption spectra and differential pulse polarography (DPP) characteristics (series 5) of these systems after exposure to 1 atm of H_2 for 30 min were unchanged compared to those of the systems under argon. The same result was obtained for [3-] with no added thiol. Finally, no detectable H_2 absorption by [3-] in a 11 mM DMF solution was found after exposure to 1 atm of H_2 for 2 h. This behavior was unchanged by addition of PhS⁻ or Et_3N, which evidently did not promote the splitting of H_2 as in reaction 2. Thus we are unable to confirm the claim of Tanaka et al.[34] that [3-] in DMF absorbs 4 mol of H_2/mol of cluster. From these observations it is concluded that, under the experimental conditions employed, reduced

---

(34) Tanaka, M.; Tanaka, K.; Tanaka, T. *Chem. Lett.* **1982**, 767.
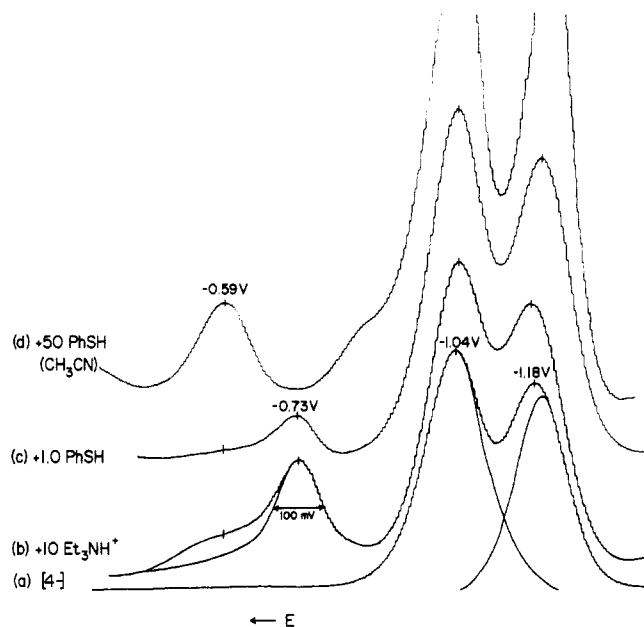
Figure 7. DP polarograms: (a) 1.98 mM [4-] in DMA, (b) +10 equiv of Et$_3$NH$^+$ after 65 min, and (c) +1.0 equiv of PhSH after 90 min; (d) 1.98 mM [4-] in acetonitrile + 50 equiv of PhSH after 1 min. Potentials were scanned from -2.0 to -0.5 V at 10 mV/s after the indicated reaction times. Smooth traces are symmetric deconvolutions of curves with the indicated peak potentials.
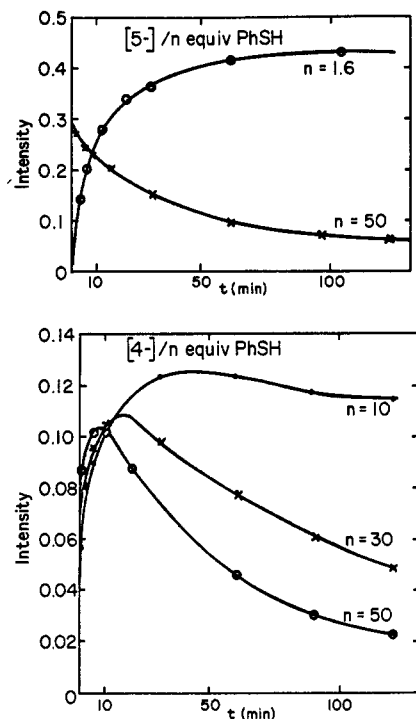

Figure 8. Rise and decay of the -0.73-V intermediate in DMA solutions: top, 0.99 mM [5-] + 1.6 and 50 equiv of PhSH; bottom, 1.98 mM [4-] + 10, 30, and 50 equiv of PhSH. Electrode potentials were held at -1.40 V ([5-]) and -1.11 V ([4-]) before potential scans and solutions were stirred 30 s before initiation of scans, which were made in the positive direction. Intensities (N_{Im}) were calculated from peak widths and half-heights and are normalized to the deconvoluted [3-]/[4-] peak area in solutions containing no PhSH ((a), Figure 7).

clusters do not react with H$_2$ and reactions 6 and 9 are not demonstrably reversible.

(d) Intermediates. When a solution of [4-] containing Et$_3$NH$^+$ or PhSH is held at a potential of ≤1.4 V and then subjected to a positive potential scan, the DP polarograms in
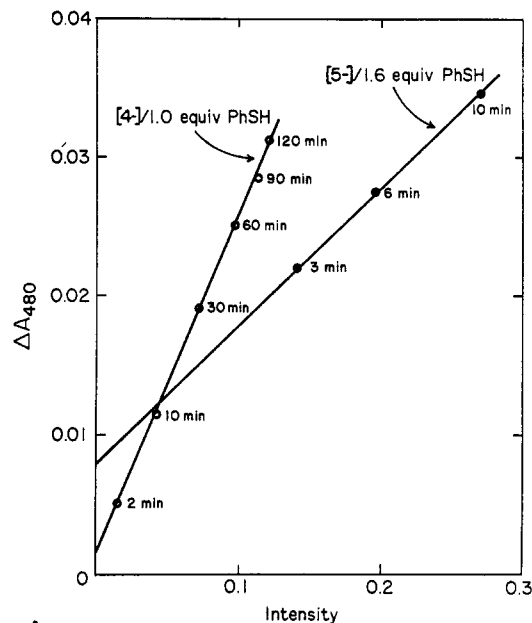
Figure 9. Plots showing the linear relationship of absorbance changes at 480 nm and the normalized intensities (N_{Im}) of the -0.73-V peak in the systems 1.98 mM [4-]/1.0 equiv of PhSH and 0.99 mM [5-]/1.6 equiv of PhSH in DMA at early periods of the reactions.

Figure 7 are observed. The potentials of the [5-]/[4-] (-1.18 V) and [4-]/[3-] (-1.04 V) processes and the ratio of their deconvoluted areas are unchanged in the presence of the protic component, and a new feature with E_p = -0.73 V appears. It is also found in [4-]/PhSH systems held at -1.1 V before potential scan (no [5-] is generated) and in [5-]/PhSH systems. The intensity of this peak is maximal under conditions of low or zero H$_2$ yields. Given in Figure 8 are plots of the intensity (area) N_{Im} of this feature, normalized to the deconvoluted area of the [4-]/[3-] process, for [4-]/PhSH and [5-]/PhSH systems at reaction times up to 120 min. In the system [5-]/1.6 equiv of PhSH N_{Im} values increase with time and H$_2$ yields are negligible. With 50 equiv of thiol these values decrease and H$_2$ yields are 30–55% (Figure 4); here reaction rates are such that only the decay of the -0.73-V feature is observed. Similar comments apply to the systems [4-]/1–50 equiv of PhSH. In the system [4-]/1.0 equiv of PhSH N_{Im} and ΔA_{480} values both increase up to 120 min and are linearly related, as shown in Figure 9   No H$_2$ was detected even after 24 h, indicating that the changes result from buildup of a reaction intermediate. Also shown is the linearity of these quantities for the system [5-]/1.6 equiv of PhSH at 3–10 min; the nonzero intercept is reproducible.

That the -0.73-V species is a reaction intermediate, hereafter designated as Im, is supported by the time and thiol equivalent dependence of N_{Im} and ΔA_{480}, and by its absence in separate solutions of PhSH, PhS$^-$, PhSSPh,[35] Et$_3$NH$^+$, H$_2$ (1 atm), and [3-]/PhSH. Its occurrence with Et$_3$NH$^+$ indicates that it does not contain PhS$^-$ or PhSH.[36]   In the foregoing [4-]/PhSH and [5-]/PhSH systems the sum of the

(35) The voltammetry of PhSH, PhS$^-$, and PhSSPh is described elsewhere: Bradbury, J. R.; Masters, A. F.; McDonnel, A. C.; Brunette, A. A.; Bond, A. M.; Wedd, A. G. *J. Am. Chem. Soc.* **1981**, *103*, 1959 and references therein.

(36) Also observed in the foregoing systems is a weak shoulder near -0.6 V (Figure 7), which decays much faster than the -0.73-V peak. This feature may represent the first electrochemically detectable intermediate but its low intensity and rapid decay precluded its study. In the system [4-]/50 equiv of PhSH in acetonitrile a prominent peak is observed at short reaction times (Figure 7). It is presumably due to the same species produced in DMA solutions. Kinetic studies of systems in acetonitrile were not pursued because of low H$_2$-evolution rates and yields (Figure 1).
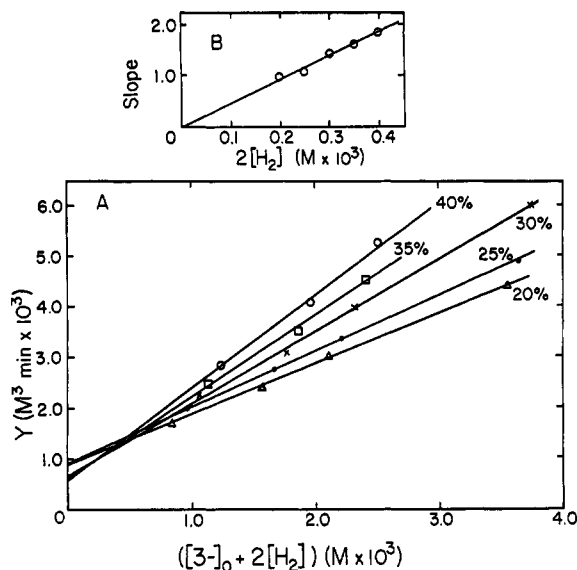
Figure 10. (A) Plots illustrating the linear relationship of Y and ($[3-]_0$ + $2[H_2]$) for the $[3-]$-inhibited systems in Figure 6. (B) Plot of the slopes of the lines in part A vs. $2[H_2]$. All lines are least-squares fits to the data.
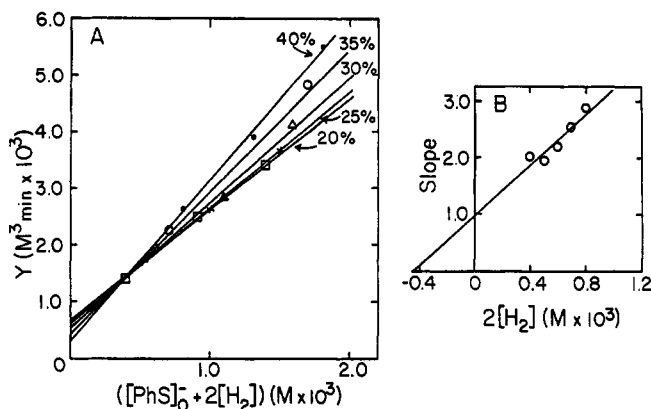
Figure 11. (A) Plots illustrating the linear relationship of Y and ($[PhS^-]_0$ + $2[H_2]$) for the PhS^--inhibited systems in Figure 6. (B) Plot of the slope of the lines in part A vs. $2[H_2]$. All lines are least-squares fits to the data.

Figure 12. (A) Plots illustrating the linear relationship of Y and $2[H_2](2[H_2] + D/C)$ for the systems $[4-]/10-50$ equiv of PhSH in Figure 5. Data points referring to the same H_2 yield occur vertically. (B) Plot of the intercepts of the lines in part A vs. $[PhSH]_0$: (—) no [PhSH] dependence of D/C; (---) horizontal axis $2[H_2](2[H_2]$ + $(k_5k_7/k_4k_6)[PhSH])$, from the D/C equation (24), where [PhSH] $\cong$ $[PhSH]_0$ because of the excess employed. All lines are least-squares fits to the data.

areas of the -1.04-V feature and 0.64 times the -0.73-V feature is constant to $\pm 1\%$, consistent with a single Im redox process in the -1.4 to -0.5 V range and consequent generation of the same intermediate from $[4-]$ or $[5-]$ and PhSH. The latter point is supported by extinction coefficients of the intermediate based on reactions 11 and 12 and the linear relationships in Figure 9 (Appendix, eq A-1–A-3). The ratio $\epsilon_{Im}(11)/\epsilon_{Im}(12b) = 0.89$, whereas $\epsilon_{Im}(11)/\epsilon_{Im}(12a) = 0.67$. It is concluded that Im is generated from $[5-]$ by reaction 11 and from $[4-]$ by reaction 12b.

Kinetic Analysis of H_2 Evolution in the $[4-]/PhSH$ System. The H_2-evolution reaction (6) for $[5-]/PhSH$ systems will inevitably generate $[4-]$ by reaction 8 at intermediary stages. Consequently, the $[4-]/PhSH$ system has been selected for kinetic analysis, although some results from the former system will be employed later in an attempt to devise a reaction mechanism. The overall reaction (9) can be formulated in terms of a number of elementary reactions such as cluster association with PhSH, cluster protonation, electron-transfer reactions of initial and intermediate clusters, hydride formation, and the final step of H_2 evolution. Various combinations of these reactions have been surveyed and the rate law for each derived under the rapid-equilibrium or steady-state approximation. The number of reaction schemes examined is too large

to allow full recountal; some are presented below. All schemes can be accommodated by the generalized rate equation (13).[37]

$$d[H_2]/dt = A[4-]^2[PhSH]^2/\{(B[3-]^2 + C[3-] + D) \times$$
$$(E[PhS^-]^2 + F[PhS^-] + G) + H[PhSH]^2 + I[PhSH]\}$$
$$(13)$$

Quantities $A–I$ are functions of elementary rate constants; $B–G$ and H, I may also contain linear multiplicative terms in [PhSH] and $[4-]$, respectively, depending on the reaction scheme.

Species concentrations are conserved in the overall reaction by eq 14, in which all intermediate concentrations are considered small under H_2-evolving conditions.

$$[4-] \cong [4-]_0 - 2[H_2]$$
$$[PhSH] \cong [PhSH]_0 - 2[H_2] \qquad (14)$$
$$[3-] \cong [3-]_0 + 2[H_2] \qquad [PhS^-] \cong [PhS^-]_0 + 2[H_2]$$

The systems $[4-]/50$ equiv of PhSH in which H_2 evolution is inhibited by $[3-]$ and $[PhS^-]$ (Figure 6) were analyzed in terms of the dependence of the quantity Y, eq 15, at constant

$$Y = \left(\frac{d[H_2]}{dt}\right)^{-1} ([4-]_0 - 2[H_2])^2([PhSH]_0 - 2[H_2])^2 \quad (15)$$

$[4-]_0$ concentration and fixed H_2 yields. Because of the excess present, [PhSH] is essentially constant. Under these conditions the effect on Y of a single concentration variable can be examined. For $[3-]$ inhibition ($[PhS^-]_0 = 0$, $[PhS^-] \cong 2[H_2]$) the linear dependence of Y on ($[3-]_0$ + $2[H_2]$) shown in Figure 10A indicates no significant contribution from $[3-]^2$; i.e., $B \cong 0$ in eq 13. Similarly, for $[PhS^-]$ inhibition ($[3-]_0 = 0$, $[3-]$

(37) In this and subsequent equations moles of H_2 formed will be written for convenience as a concentration $[H_2]$; $[3-]$, $[4-]$, and $[5-]$ are cluster concentrations, and $[-]_0$ refer to initial concentrations. The squared concentration terms in the numerator of eq 13 arise from the earlier proposal that the -0.73-V species is a reaction intermediate, generated by reaction 12b; a second PhSH molecule is required for H_2 formation.
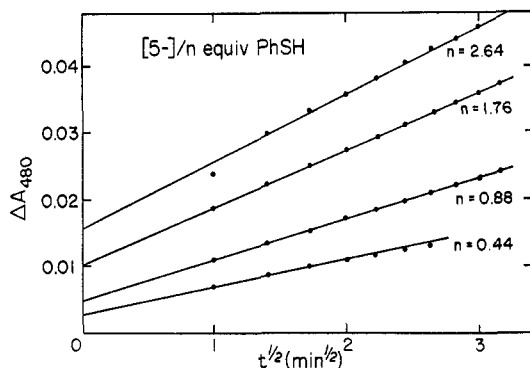
Figure 13. Plots showing the linear relationship of absorbance changes at 480 nm and (time)$^{1/2}$ due to intermediate formation at early reaction stages in the systems 1.14 mM [5-]/0.44–2.64 equiv of PhSH in DMA solutions. The lines are least-squares fits to the data.

$\simeq 2[H_2]$) the linearity in Figure 11A affords $E \simeq 0$. The zero intercept in Figure 10B, a plot of the slopes $C(2F[H_2] + G)/A$ of the lines in Figure 10A vs. $2[H_2]$, shows that $G \simeq 0$. The plot of the slopes $F(2C[H_2] + D)/A$ of the lines in Figure 11A vs. $2[H_2]$ gives $D \neq 0$, as shown in Figure 11B. The denominator of eq 13 can now be simplified to $CF([3-] + D/C)$-$[PhS^-] + H[PhSH]^2 + I[PhSH]$. For the systems [4-]/10–50 equiv PhSH in Figure 5 [3-]$_0$ = 0 and [3-] = 2[H$_2$]. Shown in Figure 12A is the linearity between Y and $2[H_2](2[H_2] + D/C)$ for constant thiol equivalents. Because the intercepts of these lines are essentially proportional to [PhSH]$_0$ (Figure 12B), the second-order term in [PhSH] is neglected. This analysis leads to the experimental rate law for H$_2$ evolution, eq 16.

$$\frac{d[H_2]}{dt} = \frac{[4-]^2[PhSH]^2}{(CF/A)([3-] + D/C)[PhS^-] + (I/A)[PhSH]} \tag{16}$$

Mechanism of H$_2$ Evolution. For the development of a chemical mechanism for H$_2$ evolution the kinetics of intermediate (Im) formation are first considered. Shown in Figure 13 is the linear dependence of ΔA_{480} on the square root of reaction times for [5-]/PhSH systems under conditions of negligible H$_2$ formation. The results have been fit to eq 17,

$$\Delta A_{480} = M + Nt^{1/2} \tag{17}$$

$$M = c_1[PhSH]_0; \quad N = c_2[PhSH]_0^{1/2}$$
$$(c_1 = 5.1 \text{ M}^{-1}, c_2 = 0.19 \text{ M}^{-1/2} \text{ min}^{-1/2}) \tag{18}$$

in which the slope and intercept are square root and linear functions, respectively, of the initial thiol concentration, eq 18 (plots omitted). No other simple time function fits the data as satisfactorily. Given the linear relationship in Figure 9, eq 17 is in effect an integrated rate equation for Im formation in the [5-]/PhSH system. For the [5-]/PhSH and [4-]/PhSH systems values of N_{Im} rise and fall (Figure 8) and H$_2$ yields increase (Figures 4 and 5) with time; both are dependent on thiol equivalents. In practice it is found that in [5-]/PhSH and [4-]/PhSH systems H$_2$-evolution rates are expressible by eq 19, a relationship based on the roughly linear dependence

$$d[H_2]/dt = K[Im][PhSH] \tag{19}$$

of the variables in Figure 14 over 20–120-min reaction times. The thiol concentration was calculated from the H atom conservation equation, [PhSH] = [PhSH]$_0$ - [Im] - 2[H$_2$], with the assumption of one H atom per Im. From these observations it is concluded that Im reacts with one PhSH molecule to form H$_2$ in both [5-] and [4-] systems. The independent establishment of Im formation from [5-] or [4-] and PhSH, described earlier, is consistent with this conclusion.
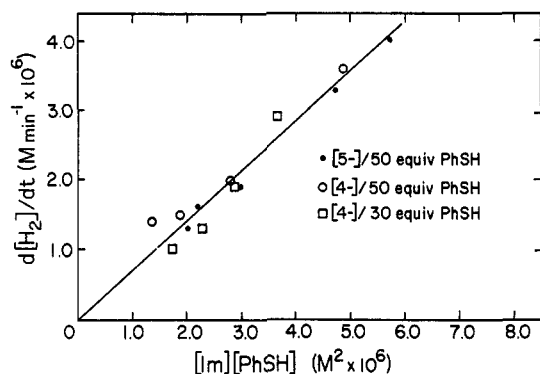

Figure 14. Plot showing linear correlation of the gradient of H$_2$ evolution and the concentration product [Im][PhSH] for [5-]/PhSH and [4-]/PhSH systems in DMA solutions. Gradients were evaluated from the yield curves in Figures 4 and 5 at 20–120-min reaction times, [Im] = $0.64N_{Im}[5-]_0$ or $0.64N_{Im}[4-]_0$, [5-]$_0$ = 0.99 mM, and [4-]$_0$ = 1.98 mM.

The mechanism of H$_2$ evolution has been approached as follows. Rate laws for Im formation in the system [5-]/PhSH have been derived for a considerable number of reaction schemes consisting of the types of elementary reactions mentioned above. The steady-state approximation was used for all other intermediates. Schemes whose rate laws do not conform to the requirements of eq 17 and 18 were discarded.[38]
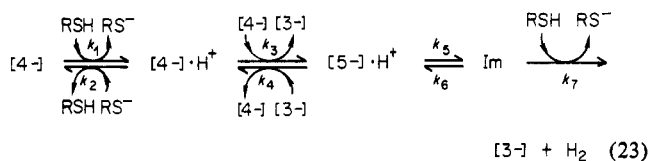
(a) [5-]/PhSH Systems. Of some nine schemes analyzed, Scheme I, containing reactions 20a–c, is the simplest representation of Im formation that is consistent with experimental results. The proposed scheme, summarized as sequence 21

$$[3-] + H_2 \tag{21}$$
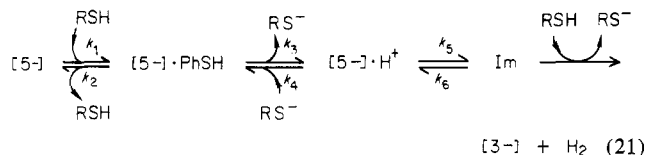
(R = Ph), consists of initial formation of a weak association complex, conversion to a protonated cluster, and Im formation. Kinetic analysis of the scheme is presented in the Appendix. The integrated rate law (eq A-9) and the expression for the absorbance change (eq A-10) satisfy the experimental requirements. These requirements are not simultaneously met by a one- or two-step generation of Im from [5-] and PhSH. Formation of [5-]·PhSH (or some other initial species) is required. Other schemes that adhere to the requirements are given in the Appendix. These include the complications of an additional intermediate and inequalities in rate constant terms that are much more difficult to justify than that proposed in arriving at Scheme I.

(b) [4-]/PhSH Systems. With use of the reaction schemes for Im formation in the preceding system as a guide, over 20 schemes were conceived and kinetically analyzed including the final step of H$_2$ evolution. These schemes met the criteria of Im generation by consumption of two [4-] and H$_2$ formation in a manner consistent with eq 19. All intermediates were treated by the steady-state approximation. The final requirement was a rate equation of the same form as the experimental rate law, eq 16. Of the various possibilities, Scheme II, consisting of reactions 22a–d and summarized as sequence 23, is considered the simplest. The process is initiated by cluster protonation and then proceeds to reduction of the protonated cluster, Im formation as in Scheme I, and H$_2$ evolution from Im by reaction with one thiol molecule. The

(38) Derivations of rate laws and their integrated forms are lengthy problems. For this reason explicit results are given (Appendix) only for those cases considered to conform most satisfactorily to experimental requirements.

$$[3-] + H_2 \quad (23)$$

	expt		
quantity	[3-] inhibition	[PhS-] inhibition	non-inhibited
CF/A, M min	$2300^{a,i}$	2300^b	2000^c
D/C, M		0.43×10^{-3} ^{d,i}	
I/A, M^2 min	$0.014^{e,h,i}$	$0.010^{f,h}$	$0.012^{g,h}$
k_1 $(M^{-1}$ min$^{-1}) = 0.14^i$		k_4/k_5k_6 $(M^{-1}$ min$^{-1}) = 0.0082$	
$k_2/k_3 = 2.8$		k_7 $(M^{-1}$ min$^{-1}) = 0.71^j$	

^{a} Evaluated from slope of Figure 10B. ^{b} Evaluated from slope of Figure 11B. ^{c} Evaluated from mean value of slopes (dashed lines) of Figure 12A. ^{d} Evaluated from x intercept of Figure 11B. ^{e} Evaluated from mean value of intercepts of Figure 10A. ^{f} Evaluated from mean value of intercepts of Figure 11A. ^{g} Evaluated from slope of Figure 12B. ^{h} For these means of evaluating I/A, $[4-] = [4-]_o$ in eq 24. ^{i} Values used in evaluating rate constants. ^{j} Slope of Figure 14.

kinetic analysis of Scheme II is given in the Appendix, where other schemes that can also satisfy the experimental rate law are included.

Correspondence between the experimental result (eq 16) and the theoretical rate law (eq A-17) requires that $k_6 \gg k_7$·[PhSH] in the unsimplified rate law (eq A-15) for Scheme II. In this case the relationships between the parameters of eq 16 and elementary rate constants are given by eq 24. The

$$\frac{CF}{A} \cong \frac{k_2k_4k_6}{k_1k_3k_5k_7} \qquad \frac{D}{C} \cong \frac{k_5k_7}{k_4k_6}[\text{PhSH}] \qquad \frac{I}{A} = \frac{[4-]}{k_1} \quad (24)$$

former were evaluated graphically from Figures 10–12,[39] and their values, with the derived rate constants, are listed in Table II. Agreement between CF/A and I/A values obtained from different experiments is quite good. Reconstruction of the time course of H_2 evolution was examined by using the derived rate constants and the integrated rate law (eq A-18). The complexity of this equation precludes a solution for $[H_2]$. Instead, experimental H_2 yields were used to calculate theoretical times for these yields. The results, plotted in Figure 5, reproduce the shapes of the yield curves and conform most closely to experiment in the 30- and 50-equiv cases. The larger divergences in the 10- and 20-equiv cases may be due to non-negligible standing concentrations of Im. In this event the conservation equations (14) used in the derivation of the integrated rate law for Scheme II become less satisfactory. As seen from Figure 8 (bottom) [Im] is not necessarily negligible in these cases.

Discussion

Several homogeneous H_2-evolving systems consisting of reduced clusters and protic reactants in purified DMA solvent have been developed in this investigation. The clusters [4-] and [5-] with 500 equiv of PhSH afford 86% and ~100% H_2 yields, respectively, after 24 h. Cluster [5-] was also found to produce H_2 from a variety of other protic sources, with the most notable result being an 83% H_2 yield from only 2 equiv of Et_3NH^+ after 24 h. The stoichiometries of H_2 formation in [5-]/PhSH and [4-]/PhSH systems were established to be those of reactions 6 and 9, respectively, and the experimental rate law for the latter system was found to be eq 16.

Under conditions of low or negligible H_2 evolution the systems [5-]/PhSH and [4-]/PhSH were found to generate a common intermediate, Im, formed from one thiol molecule and one [5-] and two [4-] species, respectively (reactions 11 and 12b). It is characterized by a redox process at −0.73 V, leads to $\Delta A_{480} \neq 0$ at short reaction times, and does not contain PhSH or PhS−. It appears to be the final kinetically resolvable species prior to H_2 formation, for which the rate law is eq 19. The reaction schemes proposed for Im formation and H_2 evolution are consistent with the experimental constraints of reactions 11 and 12b and eq 16–19, as they apply to [5-]/PhSH and [4-]/PhSH systems. Under these constraints the number of elementary steps rests entirely on kinetic analysis of reaction schemes; the species involved are not directly identified by either analysis or any experimental observations that we have been able to make. The simplest schemes consistent with experiment and the apparent rea-

sonableness of individual steps have been sought. Alternative schemes not considered below are available in the Appendix.

Formation of Im in the [5-]/PhSH case requires at least a three-step process prior to H_2 formation. Inasmuch as H^+ at some point in the sequence must be transferred to the cluster, we assume, as in Scheme I (sequence 21), initial formation of an associative species [5-]·PhSH perhaps stabilized by S–H⋯S hydrogen bonding. The second step involves proton transfer to the cluster; the initial binding site in [5-]·H^+ is presumably the most basic site, likely to be a terminal thiolate ligand. This step enjoys precedence of a sort in the proposals of initial formation of a protonated cluster in the proteolytic decomposition of $[Fe_4S_4(SR)_4]^{2-}$ [40] and in rate-limiting protonation of coordinated thiolate in $[Fe_4S_4(SR)_4]^{2-}$/R′SH ligand substitution systems.[41] The oxidized clusters 1 have been shown to undergo similar substitution reactions.[18] The next step prior to H_2 evolution is Im formation.

Deduction of the mechanistic course of H_2 evolution in the system [4-]/PhSH is a more complicated problem because of the larger number of potential species. Scheme II (sequence 23) is perhaps the simplest; it involves three steps for Im formation, does not necessitate a kinetically significant associative species, and presents the fully reduced protonated cluster [5-]·H^+ as the immediate precursor to Im. At least the first two steps leading to Im are likely to be endothermic. In particular, $k_4 \gg k_3$ is probable. While the forward reaction (k_3) should proceed to an extent on the reasonable assumption that a protonated cluster is reducible by its unprotonated form, the reverse reaction enjoys a driving force such as is associated with comproportion reaction 8. The occurrence of several unfavorable steps can account for the large excesses of thiol required for H_2 yields of, e.g., >20% in reaction times longer than ~2 h (Figures 1 and 5). The reaction sequence is driven by the previously noted irreversibility of the final step; of the derived rate constants k_7 is the largest. The integrated rate law for Scheme II is fairly successful in reproducing the time course of H_2 evolution in the presence of large excesses of PhSH (Figure 5).

In all reaction schemes intermediate species, except Im, have been formulated as double cubanes. Several qualifying observations are noted. With 2,4,6-$C_6H_2D_3SH$ under H_2-evolving conditions the systems [5-]/10–100 equiv of thiol in DMA were allowed to react for 2 h, after which the solutions were treated as described in Figure 2. ^1H NMR spectra

(39) Note from Figure 12B that the argument excluding a [PhSH]^2 term in the denominator of eq 16 still holds upon recognition that Scheme II produces a linear dependence of D/C on [PhSH] (eq 24).

(40) Bruice, T. C.; Maskiewicz, R.; Job, R. *Proc. Natl. Acad. Sci. U.S.A.* **1975**, *72*, 231.

(41) Dukes, G. R.; Holm, R. H. *J. Am. Chem. Soc.* **1975**, *97*, 528.

revealed the expected exchange of terminal ligands[18] and a smaller but definite incorporation of PhS^--d_3 in the bridge, as shown by the increasing intensity ratio $m\text{-}H_b/p\text{-}H_b$ with increasing thiol equivalents. Previously, the oxidized cluster $[Mo_2Fe_6S_8(SEt)_9]^{3-}$ was found to be unreactive in the bridge positions toward small excesses of acetyl chloride and PhSH.[18] The present finding demonstrates Mo–S bridge bond breaking and bridge ligands as a possible protonation site but does not require that a bridge-cleaved species lie on the reaction pathway. The most attractive formulation of Im is $[3-]\cdot H^-$, in which internal electron transfer of $[5-]\cdot H^+$ generates a hydride ligand, stabilized at a metal site. Such a process is analogous to reaction 3. The Im redox reaction at -0.73 V is ~ 0.70 V more negative than the $[3-]/[2-]$ potential, and reduction steps characteristic of the double-cubane structure are not observed at ≤ -1.4 V. These results provide no prima facie evidence for such a structure, but the effect of cluster-bound H^+ and H^- on potentials is experimentally unknown. The chemical test for a hydride intermediate, viz., incubation of $[3-]/PhSH$ in the presence of D_2 and search for HD and D_2, has not been attempted. The lack of reversibility of reactions 6 and 9, by the criterion of no detectable H_2 uptake, does not remove the possibility of formation of small concentrations of a hydride intermediate by a reaction such as (2) (B = coordinated PhS^-).

Core extrusion results for hydrogenases containing 8–12 Fe atoms per functional unit point to the presence of Fe_4S_4 clusters.[42-44] In the absence of other metal-containing components one or more of these clusters in a reduced state presumably acts as the catalytic site for reaction 1. The clusters 1–3 cannot be accurate models for the catalytic sites of hydrogenases, for these enzymes are not known to contain molybdenum. However, they may simulate one important feature of a multicluster enzyme: appropriate juxtaposition of two weakly coupled reduced clusters allows a (perhaps concerted) two-electron transfer to a protic substrate. This is expressed by the k_5 step in Scheme II and by corresponding steps in alternative schemes (Appendix). Subsequent protonation of a transient hydride, perhaps here stabilized at an Fe site, completes the process, which is formally analogous to the reactions (3).[45] Formation of H_2 in $[Fe_4S_4(SPh)_4]^{3-}/PhSH$ systems in DMA provides evidence that reduced clusters of this type do have intrinsic hydrogenase-like activity. However, the relatively low yields (Figure 1) have discouraged a detailed kinetic study. A similar situation has been encountered in $[Fe_4S_4(SPh)_4]^{3-}/C_2H_2/HOAc$ systems,[48] where ethylene yields did not exceed $\sim 60\%$ on the basis of reduced cluster although the cluster component was fully oxidized. Doubly reduced clusters generally may be more effective reductants of two-electron substrates than singly reduced clusters. The results of this investigation define several cases where this is true.

(42) Gillum, W. O.; Mortenson, L. E.; Chen, J.-S.; Holm, R. H. *J. Am. Chem. Soc.* **1977**, *99*, 584.
(43) Hatchikian, E. C.; Bruschi, M.; LeGall, J. *Biochem. Biophys. Res. Commun.* **1978**, *82*, 451.
(44) Okura, I.; Nakamura, K.-I.; Nakamura, S. *J. Mol. Catal.* **1979**, *6*, 311.
(45) If in the newly discovered Ni-containing hydrogenases[4] the Ni atom is the catalytic site, a prospect entertained for a *D. gigas* hydrogenase[46] (1Ni, 12Fe/S), the Fe–S clusters fulfill an electron-transfer function only. In H_2-evolving dithionite/ferredoxin/hydrogenase systems the clusters 1 and $[Fe_4S_4(SR)_4]^{2-}$ have been shown to replace ferredoxin, but not hydrogenase, with retention of activity.[47]
(46) Cammack, R.; Patel, D.; Aguirre, R.; Hatchikian, E. C. *FEBS Lett.* **1982**, *142*, 289.
(47) Adams, M. W. W.; Rao, K. K.; Hall, D. O.; Christou, G.; Garner, C. D. *Biochim. Biophys. Acta* **1980**, *589*, 1.
(48) McMillan, R. S.; Renaud, J.; Reynolds, J. G.; Holm, R. H. *J. Inorg. Biochem.* **1979**, *11*, 213.

Appendix

Extinction coefficients of the intermediate are given by eq A-1–A-3, where $[-]$ = molar concentration, l = path length

reaction 11: $\epsilon_{Im}^{480}(11) = \epsilon_{5-}^{480} + \Delta A_{480}/0.64 N_{Im}[5-]l$ (A-1)

reaction 12a: $\epsilon_{Im}^{480}(12a) = \epsilon_{4-}^{480} + \Delta A_{480}/0.64 N_{Im}[4-]l$ (A-2)

reaction 12b: $\epsilon_{Im}^{480}(12b) =$

$2\epsilon_{4-}^{480} - \epsilon_{3-}^{480} + \Delta A_{480}/0.64 N_{Im}[4-]l$ (A-3)

(cm), $\epsilon_{3-}^{480} = 30\,200$ M^{-1} cm^{-1}, $\epsilon_{4-}^{480} = 20\,300$ M^{-1} cm^{-1}, and $\epsilon_{5-}^{480} = 10\,300$ M^{-1} cm^{-1}. Values of $\Delta A_{480}/N_{Im}$ were obtained from the gradients of the plots in Figure 9.

Kinetic Analysis of Scheme I. On the basis of the steady-state approximation for reactions 20a and 20b the rate of Im formation is given by eq A-4. Substitution using the con-

$$\frac{d[Im]}{dt} = \frac{k_1 k_3 k_5[5-][PhSH] - k_2 k_4 k_6[PhS^-][Im]}{k_2 k_4[PhS^-] + (k_2 + k_3)k_5}$$ (A-4)

servation equations (A-5) gives eq A-6. Rearrangement of

$$[5-]_0 \cong [5-] + [5{-}\cdot PhSH] + [Im]$$

$$[PhSH]_0 \cong [PhSH] + [5{-}\cdot PhSH] + [Im]$$ (A-5)

$$[PhSH]_0 \cong [PhS^-] + [5{-}\cdot PhSH] + [PhSH]$$

$d[Im]/dt \cong (k_1 k_3 k_5/k_2 k_4)\{(([5-]_0 - [5{-}\cdot PhSH] - [Im]) \times$

$([PhSH]_0 - [5{-}\cdot PhSH] - [Im]) - k_2 k_4 k_6[Im]^2)/$

$([Im] + k_5/k_4 + k_3 k_5/k_2 k_4)\}$ (A-6)

eq A-6 leads to eq A-7 in which α and β are mathematically

$$\frac{d[Im]}{dt} \cong$$

$$\frac{k_1 k_3 k_5}{k_2 k_4}\left[\frac{\left(1 - \frac{k_2 k_4 k_6}{k_1 k_3 k_5}\right)([Im] - \alpha)([Im] - \beta)}{[Im] + k_5/k_4 + k_3 k_5/k_2 k_4}\right]$$ (A-7)

convenient expressions containing rate constants and concentrations (except $[Im]$). Integration over the limits $(0, t)$ and $(0, [Im])$ gives eq A-8 in which the right-hand side was sim-

$$\left(\frac{k_1 k_3 k_5}{k_2 k_4} - k_6\right)t =$$

$$\frac{[Im]^2}{2\alpha\beta} + \left(\frac{k_5}{k_4} + \frac{k_3 k_5}{k_2 k_4}\right)\left(\frac{[Im]}{\alpha\beta} + \frac{(\beta + \alpha)[Im]^2}{\alpha^2\beta^2}\right)$$ (A-8)

plified by use of the expansion $\ln(1 - y) = -\sum_{n=1}^{\infty} y^n/n$ ($|y| < 1$) to second order. The substitution

$$\alpha\beta = \left(\frac{k_1 k_3 k_5}{k_1 k_3 k_5 - k_2 k_4 k_6}\right)([5-]_0 - [5{-}\cdot PhSH]) \times$$

$$([PhSH]_0 - [5{-}\cdot PhSH])$$

with $[5{-}\cdot PhSH] \ll [5-]_0$, $[PhSH]_0$ affords the rate equation (A-9), under the condition that $[Im]^2/2\alpha\beta \gg$ product term

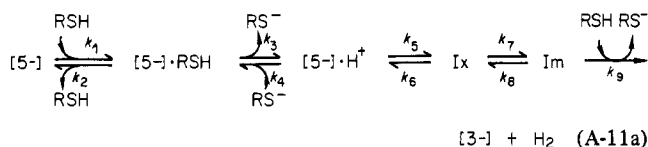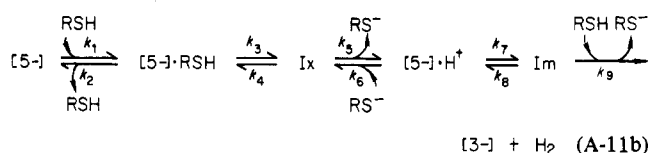$$[Im] \cong \left(\frac{2k_1 k_3 k_5}{k_2 k_4}[5-]_0[PhSH]_0 t\right)^{1/2}$$ (A-9)

in the right-hand side of eq A-8. This corresponds to $k_2 k_4[PhS^-] \gg (k_2 + k_3)k_5$ in eq A-4, i.e., to the rapid-equilibrium treatment, in which constant intermediate concentrations are rapidly established in reactions 20a and 20b. The absorbance change due to Im formation is given by eq A-10; $[5{-}\cdot PhSH] \cong k_1[5-]_0[PhSH]_0/k_2$ prior to the onset of Im formation from the rapid equilibrium approximation of reaction 20a. When

$$\Delta A \cong (\epsilon_{Im} - \epsilon_{5-})l\left(\frac{2k_1k_3k_5}{k_2k_4}[5-]_0[PhSH]_0 t\right)^{1/2} +$$

$$(\epsilon_{5\rightarrow PhSH} - \epsilon_{5-})l\frac{k_1}{k_2}[5-]_0[PhSH]_0 \quad (A\text{-}10)$$

analyzed similarly, two other schemes for Im formation, shown by (A-11) (R = Ph, Ix = second intermediate), meet the requirements of eq 17 and 18 under the stated assumptions.

$$[5\text{-}] \underset{\overset{RSH}{k_2}}{\overset{\overset{RSH}{k_1}}{\rightleftharpoons}} [5\text{-}]\cdot RSH \underset{\overset{RS^-}{k_4}}{\overset{\overset{RS^-}{k_3}}{\rightleftharpoons}} [5\text{-}]\cdot H^+ \underset{k_6}{\overset{k_5}{\rightleftharpoons}} Ix \underset{k_8}{\overset{k_7}{\rightleftharpoons}} Im \overset{RSH\ RS^-}{\underset{k_9}{\rightharpoonup}}$$

$$[3\text{-}] + H_2 \quad (A\text{-}11a)$$

$$k_2k_4(k_6 + k_7) \gg (k_2 + k_3)k_5k_7$$

$$[5\text{-}] \underset{\overset{RSH}{k_2}}{\overset{\overset{RSH}{k_1}}{\rightleftharpoons}} [5\text{-}]\cdot RSH \underset{k_4}{\overset{k_3}{\rightleftharpoons}} Ix \underset{\overset{RS^-}{k_6}}{\overset{\overset{RS^-}{k_5}}{\rightleftharpoons}} [5\text{-}]\cdot H^+ \underset{k_8}{\overset{k_7}{\rightleftharpoons}} Im \overset{RSH\ RS^-}{\underset{k_9}{\rightharpoonup}}$$

$$[3\text{-}] + H_2 \quad (A\text{-}11b)$$

$$k_2k_4k_6[PhS^-] \gg (k_2k_4 + k_2k_5 + k_3k_5)k_7$$

Kinetic Analysis of Scheme II. The steady-state approximation for all intermediates leads to eq A-12–A-14. Elimination of $[4\rightarrow H^+]$ and $[5\rightarrow H^+]$ by use of these equations and

$$[4\rightarrow H^+] \cong \frac{k_1[4\text{-}][PhSH] + k_4[5\rightarrow H^+][3\text{-}]}{k_2[PhS^-] + k_3[4\text{-}]} \quad (A\text{-}12)$$

$$[5\rightarrow H^+] \cong \frac{k_3[4\rightarrow H^+][4\text{-}] + k_6[Im]}{k_4[3\text{-}] + k_5} \quad (A\text{-}13)$$

$$[Im] \cong \frac{k_5[5\rightarrow H^+]}{k_6 + k_7[PhSH]} \quad (A\text{-}14)$$

setting $k_7 = K$ in eq 19 produce the rate equation (A-15).

$$d[H_2]/dt = k_1k_3k_5k_7[4\text{-}]^2[PhSH]^2/\alpha \quad (A\text{-}15)$$

$$\alpha = k_2k_4(k_6 + k_7[PhSH])$$

$$\left([3\text{-}] + \frac{k_5k_7[PhSH]}{k_4(k_6 + k_7[PhSH])}\right)[PhS^-] + k_3k_5k_7[4\text{-}][PhSH]$$

Comparison with the experimental rate law, eq 16, shows the relationships of eq A-16. An experimental result is that

$$\frac{CF}{A} = \frac{k_2k_4(k_6 + k_7[PhSH])}{k_1k_3k_5k_7} \qquad \frac{I}{A} = \frac{[4\text{-}]}{k_1}$$

$$\frac{D}{C} = \frac{k_5k_7[PhSH]}{k_4(k_6 + k_7[PhSH])} \quad (A\text{-}16)$$

CF/A, which may be obtained from the slopes of Figure 12A, is almost independent of [PhSH]. This supports the approximation $k_6 \gg k_7[PhSH]$ and simplification of eq A-15 to eq A-17. Substitution using the conservation equations (14) and
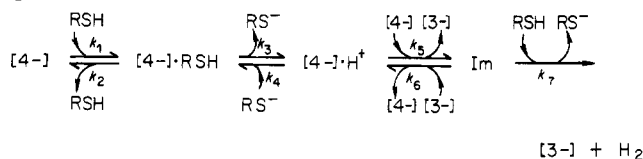
$$d[H_2]/dt \cong k_1k_3k_5k_7[4\text{-}]^2[PhSH]^2/\left\{k_2k_4k_6\left([3\text{-}] + \right.\right.$$

$$\left.\left.\frac{k_5k_7}{k_4k_6}[PhSH]\right)[PhS^-] + k_3k_5k_7[4\text{-}][PhSH]\right\} \quad (A\text{-}17)$$

integration over $(0, t)$ and $(0, [H_2])$ afford the rate law eq A-18, where $\sigma = ([PhSH]_0 - [4\text{-}]_0)/[4\text{-}]_0$, $h = 2[H_2]/[4\text{-}]_0$
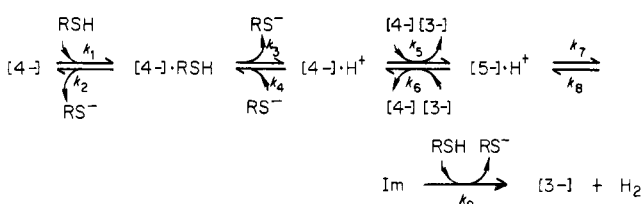
(fractional H_2 yield), and $Q = (\sigma + 1 - h)/(\sigma + 1)(1 - h)$.

$$t = \frac{k_2k_4k_6}{k_1k_3k_5k_7}\left\{\frac{[3\text{-}]_0[PhS^-]_0}{2\sigma^2[4\text{-}]_0^3}\left[-\frac{1}{\sigma + 1} + \right.\right.$$

$$\left.\frac{1}{\sigma + 1 - h} + \frac{h}{1 - h} - \frac{2}{\sigma}\ln Q\right] +$$

$$\frac{[3\text{-}]_0 + [PhS^-]_0}{2\sigma^2[4\text{-}]_0^2}\left[\frac{h}{\sigma + 1 - h} + \frac{h}{1 - h} - \frac{\sigma + 2}{\sigma}\ln Q\right] +$$

$$\frac{1}{2\sigma^2[4\text{-}]_0}\left[\frac{h}{1 - h} + \frac{(\sigma + 1)h}{\sigma + 1 - h} - \frac{2(\sigma + 1)}{\sigma}\ln Q\right]\right\} +$$

$$\frac{k_2}{k_1k_3}\left\{\frac{[PhS^-]_0}{2\sigma[4\text{-}]_0^2}\left[\frac{h}{1 - h} - \frac{1}{\sigma}\ln Q\right] + \frac{1}{2\sigma[4\text{-}]_0}\left[\frac{h}{1 - h} - \right.\right.$$

$$\left.\left.\frac{\sigma + 1}{\sigma}\ln Q\right]\right\} + \frac{1}{2k_1\sigma[4\text{-}]_0}\ln Q \quad (A\text{-}18)$$

When analyzed by using the steady-state approximation, four other schemes can yield rate laws of the form of eq 16. These are shown below, together with rate laws for the two simplest cases. Equation A-19 requires no approximation, and that required to bring eq A-20 into conformance with eq 16 is analogous to that for Scheme II. Rate laws for the last two schemes require more complicated approximations that are difficult to justify; for this reason the rate expressions are omitted.[38] Also excluded because of their complexity are kinetically acceptable schemes having branched reaction sequences.
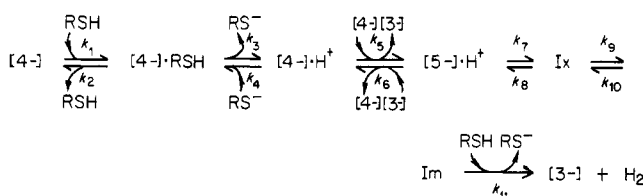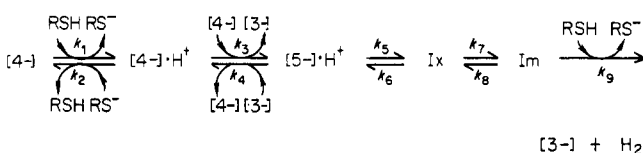
$$[4\text{-}] \underset{\overset{RSH}{k_2}}{\overset{\overset{RSH}{k_1}}{\rightleftharpoons}} [4\text{-}]\cdot RSH \underset{\overset{RS^-}{k_4}}{\overset{\overset{RS^-}{k_3}}{\rightleftharpoons}} [4\text{-}]\cdot H^+ \underset{\overset{[4\text{-}]\ [3\text{-}]}{k_6}}{\overset{\overset{[4\text{-}]\ [3\text{-}]}{k_5}}{\rightleftharpoons}} Im \overset{RSH\ RS^-}{\underset{k_7}{\rightharpoonup}}$$

$$[3\text{-}] + H_2$$

$$d[H_2]/dt = k_1k_3k_5k_7[4\text{-}]^2[PhSH]^2/\{k_2k_4(k_6[3\text{-}] + k_7[PhSH])[PhS^-] + (k_2 + k_3)k_5k_7[4\text{-}][PhSH]\} \quad (A\text{-}19)$$

$$[4\text{-}] \underset{\overset{RSH}{k_2}}{\overset{\overset{RSH}{k_1}}{\rightleftharpoons}} [4\text{-}]\cdot RSH \underset{\overset{RS^-}{k_4}}{\overset{\overset{RS^-}{k_3}}{\rightleftharpoons}} [4\text{-}]\cdot H^+ \underset{\overset{[4\text{-}]\ [3\text{-}]}{k_6}}{\overset{\overset{[4\text{-}]\ [3\text{-}]}{k_5}}{\rightleftharpoons}} [5\text{-}]\cdot H^+ \underset{k_8}{\overset{k_7}{\rightleftharpoons}}$$

$$Im \overset{RSH\ RS^-}{\underset{k_9}{\rightharpoonup}} [3\text{-}] + H_2$$

$$d[H_2]/dt = k_1k_3k_5k_7k_9[4\text{-}]^2[PhSH]^2/\alpha \quad (A\text{-}20)$$

$$\alpha = k_2k_4\{k_6(k_8 + k_9[PhSH])[3\text{-}] + k_7k_9[PhSH]\} \times$$

$$[PhS^-] + (k_2 + k_3)k_5k_7k_9[4\text{-}][PhSH]$$

$$k_8 \gg k_9[PhSH]$$

$$[4\text{-}] \underset{\overset{RSH\ RS^-}{k_2}}{\overset{\overset{RSH\ RS^-}{k_1}}{\rightleftharpoons}} [4\text{-}]\cdot H^+ \underset{\overset{[4\text{-}]\ [3\text{-}]}{k_4}}{\overset{\overset{[4\text{-}]\ [3\text{-}]}{k_3}}{\rightleftharpoons}} [5\text{-}]\cdot H^+ \underset{k_6}{\overset{k_5}{\rightleftharpoons}} Ix \underset{k_8}{\overset{k_7}{\rightleftharpoons}} Im \overset{RSH\ RS^-}{\underset{k_9}{\rightharpoonup}}$$

$$[3\text{-}] + H_2$$

$$[4\text{-}] \underset{\overset{RSH}{k_2}}{\overset{\overset{RSH}{k_1}}{\rightleftharpoons}} [4\text{-}]\cdot RSH \underset{\overset{RS^-}{k_4}}{\overset{\overset{RS^-}{k_3}}{\rightleftharpoons}} [4\text{-}]\cdot H^+ \underset{\overset{[4\text{-}]\ [3\text{-}]}{k_6}}{\overset{\overset{[4\text{-}]\ [3\text{-}]}{k_5}}{\rightleftharpoons}} [5\text{-}]\cdot H^+ \underset{k_8}{\overset{k_7}{\rightleftharpoons}} Ix \underset{k_{10}}{\overset{k_9}{\rightleftharpoons}}$$

$$Im \overset{RSH\ RS^-}{\underset{k_{11}}{\rightharpoonup}} [3\text{-}] + H_2$$